Electron-phonon interaction and cyclotron resonance in lead

I. Ya. Krasnopolin and M. S. Khaĭkin
Institute of Physics Problems, USSR Academy of Sciences
(Submitted December 21, 1972)
Zh. Eksp. Teor. Fiz. **64**, 1750-1761 (May 1973)

Electron and hole cyclotron resonance is studied in lead single crystals with a residual relaxation time $\tau_0 \approx 1-2$ nsec in the 0.4 to 4.2°K temperature range and at frequencies of 9.25, 19.2 and 75.9 GHz. The effective masses of current carriers are found to increase with the temperature as T^2 and $\Delta m^*(4.2°K)/m^*(0) \approx 2\%$, in accordance with the theory of electron-phonon interaction at finite temperatures. The electron and hole relaxation time at the central sections of the Fermi surface and its temperature dependence are determined by analyzing the shape of the high-resolution cyclotron resonance line ($\omega\tau \approx 50-400$). The inverse relaxation time $\tau_{ep}^{-1} = aT^3$, the coefficient a being twice as high for holes as for electrons. Additional damping of quasiparticles is manifest at 75.9 GHz (for temperatures such that $kT < \hbar\omega$ the inverse relaxation time varies as $\sim T^2$). This damping is due to removal of electrons and holes from the Fermi surface by $\sim\hbar\omega$. The theoretical value of the additional damping is lower than that observed experimentally.

Electron-phonon interaction leads to a change in the energy spectrum of the conduction electrons of a metal near the Fermi surface, at a depth $\sim\omega_D$ (ω_D is the characteristic frequency of the phonon spectrum). In theory, this circumstance makes it necessary to renormalize the electron spectrum[1]. The indicated distortion of the energy spectrum is manifest in a decrease in the electron velocity on the Fermi surface and in a corresponding decrease on the low-temperature part of the electronic heat capacity of metals[2]. On the other hand, experiments on cyclotron resonance (CR) have established that the effective masses of the electrons also exceed systematically the masses obtained on the basis of band calculations[2,3]. The effective mass of the electrons can be represented in the form

$$m^* = m_b(1+\lambda), \qquad (1)$$

where λ is a coefficient characterizing the electron-phonon interaction, m_b is the mass due to the band structure, and the contribution made by the Coulomb electron-electron interaction for transition metals (in particular, lead) is small in accordance with the calculations[2]. We note that the quantity λ affects strongly the temperature of the transition of a metal into the superconducting state, and in superconductors with strong coupling ($\lambda \sim 1$) the parameters of the electron-phonon interaction, averaged over the Fermi surface, can be determined from measurements of the current-voltage characteristics of tunnel junctions[4].

Thus, measurement of m* with the aid of CR in metals is one of the important methods of investigating the energy spectrum of electrons interacting with phonons in a real metal. It must be emphasized here that in the study of CR one investigates properties of perfectly defined groups of electrons with an extremal effective mass.

With increasing temperature in a system of interacting Fermi particles, in view of the fact that the energy of the quasiparticles is a functional of the distribution function, the energy of each individual quasiparticle also changes. This leads to an additional contribution to the heat capacity of the system[1]. Éliashberg[5] predicted for the heat capacity of metals a term that is connected with the electron-phonon interaction and depends on the temperature like $T^3 \ln T$. A numerical calculation of the magnitude of the effect in sodium[6], in lead, and in mercury[7] has shown that it is difficult to separate it from the total specific heat. Grimvall[7] has also shown that the variation of λ with the temperature should lead to an increase of the effective mass, like $m^* \propto T^2$ in lead and in mercury, and that in the temperature interval 0—4°K this change is $\Delta m^*/m^* \approx 3\%$.

The effective mass of electrons can be measured with high accuracy (better than 0.1%) by the CR method in samples with high values of $\omega\tau$. Observation of the indicated effect in lead has already been reported earlier[8]. Similar experiments were performed independently on lead[9], mercury[10], zinc[11], and indium[12]. The effective mass apparently does not increase with temperature in semimetals[13]: No change of m* with accuracy ~0.05%, was observed in antimony in the interval T = 2—8°K.

In the study of the dependence of the high-resolution CR spectra on the temperature it is possible to extract from an analysis of the line shape also another quantity that characterizes quasiparticle interaction, namely, the lifetime of the quasiparticles as a function of the temperature and of the frequency of the electromagnetic radiation.

We have investigated in detail, by the CR method, the temperature dependences on the effective mass and on the relaxation times of the two main group of carriers in lead, namely the electrons of the third zone and the holes of the second zone, at frequencies 9.25, 19.2, and 75.9 GHz.

EXPERIMENT

We investigated three lead single crystals in the form of discs of 17.8 mm diam: Pb I and Pb II, of thickness 1 mm, and Pb III of thickness 0.2 mm. The normal to the flat surface of the Pb I sample made an angle ~20° with the [001] axis, while the [110] axis was in the plane of the sample[1)]. The samples Pb II and Pb III were grown in the setup described in[14]. The original material was lead of brand S-0000[2)]. In Pb II, the normal to the flat surface made an angle ~11°30′ with the [011] axis, and the $[0\bar{1}1]$ axis made an angle ~10° with the plane of the sample. The flat part of the

Pb III single crystal coincided within ~1° with the (011) plane.

The purity and perfection of the investigated single crystal are characterized by a residual relaxation time, which amounted, for the electrons on the central section of the tube in the third zone, to

$$\tau_0^{I} = 1.2 \cdot 10^{-9} \text{ sec}, \quad \tau_0^{II} = 2.5 \cdot 10^{-9} \text{ sec}, \quad \tau_0^{III} = 2 \cdot 10^{-9} \text{ sec}.$$

The CR was measured at frequencies 19.2 GHz (Pb I)[8], 9.25 and 75.9 GHz (Pb II), and 9.88 GHz (Pb III). At the two lowest frequencies, the sample was placed freely on a quartz substrate in a strip resonator connected in the feedback circuit of a TWT self-oscillator[15]. We measured either the low-frequency component (at the magnetic-field modulation frequency 12 Hz) of the generation amplitude near threshold, or the deviation of the generator frequency[15]. The resonator with the sample were placed in a cryostat cooled with liquid He^3 (Pb I and Pb III) or with liquid He^4 (Pb II). A magnetic field up to ~10 kOe was produced with an electromagnet; the field intensity was measured with a Hall pickup calibrated with a NMR magnetometer with running water[16] for each recording of the investigated section of the CR spectrum; the accuracy with which the magnetic field was measured was better than 0.1%. The magnetic field was made parallel to the flat surface of the sample with accuracy ~5′ as determined by the splitting of the CR lines on the non-central sections of the Fermi surface.

The experiments at 75.9 GHz (Pb II) were performed in a cryostat (Fig. 1) with a superconducting solenoid[17] (outside diameter 110 mm, height 216 mm, inside diameter 54 mm), made of a 7-lead cable KSI 030/0.05. At the maximum current ~160 A, a magnetic field ~53 kOe was produced at the center of the solenoid (T = 4.2°K). The NMR magnetometer[16] was used to calibrate the magnetic field intensity at the center of the solenoid against the current, and also to check on its homogeneity. The constant of the solenoid fields 10–50 kOe was C = 333.5 ± 0.3 Oe/A, and the homogeneity of the magnetic field in a sphere of radius ~1 cm was $\sim 10^{-4}$. The solenoid was fed from a stabilized current source[18] up to 180 A, the long-time (~10 min) stability of the current was better than 10^{-4}, and the level of the current pulsations was $\sim 10^{-6}$ at 1 kHz frequency, the current through the solenoid was determined from the voltage drop across standard resistance coils of 0.001 or 0.00005 Ω with a Solartron digital voltmeter, with accuracy 0.05%. The constructions of the solenoid and of the power supply made it possible to investigate narrow CR lines with resolution up to 10^{-4}.

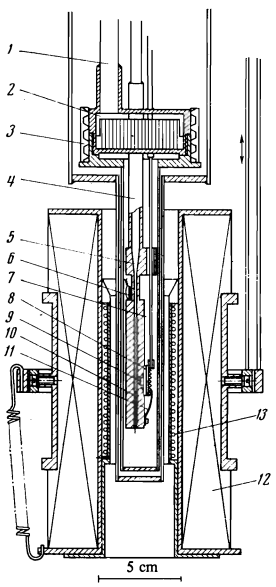

FIG. 1. Low-temperature part of the instrument for the investigation of CR at 75.9 GHz: 1–tube for pumping the He^3, 2–He^3 liquefaction chamber, 3–teflon ring sealing the vacuum vessel, 4–tubular copper waveguides, 5–transition piece to rectangular waveguide 3.6 × 1.8 mm, 6–resistance thermometer, 7–drive for rotating the sample, 8–sample, 9–resonator cavity, 10–piston for tuning the coupling, 11–spring for securing the sample, 12–solenoid, 13–coil for modulating the magnetic field.

A metallic cryostat with a measuring resonator 9, one of the walls of which was the sample 8, was placed in the opening of the solenoid. In view of the need for placing the sample vertically in the resonator, the crystal was secured with a flat bronze spring 11. This fastening deteriorated the quality of the sample, reducing τ_0^{II} to a value 0.7×10^{-9} sec. Oscillations of TM_{110} type were excited with a Q ~ 5000–7000 in the cylindrical through resonator at low temperatures.

The change of the surface resistances of the sample while the magnetic field was scanned was determined from the change in the power transmission coefficient through the resonator, which was weakly coupled to the waveguide lines. The frequency-modulated microwave signal from a backward-wave tube, passing through the resonator, was modulated in amplitude and detected with a microwave detector. The direct-amplification circuit with a selective amplifier and a synchronized detector registered, during the passage of the CR line over the magnetic field, the low-frequency component (at the magnetic-field modulation frequency 12 Hz) of the amplitude of the signal passing through the resonator. The sensitivity of the circuit made it possible to investigate the CR lines in lead for two principal orbits: electronic ζ on the central section of the tube in the third band, and hole ψ on the central section of the Fermi surface in the second zone[3], characterized by the parameter $\omega\tau \approx 50$–400.

The resonator with the sample was suspended on copper tubular waveguides 4 in a vacuum-type vessel, the upper cover of which was the bottom of chamber 2 for the liquefaction of the He^3. To improve the heat exchange, gaseous He^3 was admitted into the vessel at T ≈ 80°K and at a pressure ~10 mm Hg. By varying the vapor pressure over the liquid He^3 it was possible to vary the sample temperature from 0.4 to 3°K. The temperature was determined from the vapor pressure of the He^3 and monitored against the readings of an Allen-Bradley carbon resistor 6 glued to the resonator. To prevent the sample from overheating, the measurements at T ≤ 1°K were performed at the lowest possible microwave power level in the resonator, <100 μW, and at a modulation field amplitude $\tilde{H} \approx 10$ Oe (at a line width $\Delta H \approx 100$ Oe). Test variations of the microwave power level or of the modulation-field amplitude by a factor 2–3 did not change the width or the position of the SR line. For the measurements at 3°K ≤ T ≤ 4.2°K, He^4 was made to flow into the vacuum jacket of the cryostat with the He^3 chamber, so that when the He^4 was poured into the volume with the superconducting solenoid, the gaseous He^4 condensed in the jacket and the vacuum vessel with the resonator was in direct thermal contact with the He^4 bath. The temperature was measured in this case against the He^4 vapor pressure and with the Allen-Bradley resistor.

MEASUREMENT RESULTS

Figure 2 shows the CR lines ζ on the central section of the electronic tube in the third zone of the Fermi

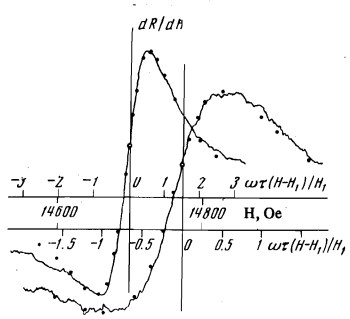

FIG. 2. CR lines of first order at 75.9 GHz, angle ≈ 7° between H and [0$\bar{1}$1]. Left curve–T = 0.86°K, $\omega\tau$ = 306; right curve–T = 2.32°K, $\omega\tau$ = 134; ●–calculation by formula (2), ○–position of resonant value of H_1.

surface at 75.9 GHz with the magnetic field H making an angle ~7° with the [0$\bar{1}$1] axis of the crystal: $m^*_\zeta(0)/m_0 = 0.541 \pm 0.001$. The plots were obtained at two temperatures, 0.86 and 2.32°K. The reduction of such plots (a typical example at 19.2 GHz can be found in our preceding paper[8]) was by means of the Chambers formulas[19]. The use of these formulas is justified because: 1) in our experiments the change of the surface resistance at resonance constitutes a small part of its values off resonance ($\Delta R/R \sim 10^{-3}$ even at $\omega\tau \approx 400$). This may be due both to the relative smallness of the number of resonating electrons (nonsphericity and multiply-connected character of the Fermi surface) and with the partial specularity of the reflection of the electrons from the sample surface[20,21]. We note that resonance on the hole orbit ψ has an intensity smaller by a factor 2–3, and this causes, in particular, the smaller temperature interval in which it was possible to measure $m^*(T)$ and $\tau_\psi(T)$; 2) the parameter $\omega\tau$ in our experiments ranged from 300–400 to 50 at f = 75.9 GHz, from 150 to 40 at f = 19.2 GHz, and from 80 to 30 at f = 9.25 GHz in the investigated temperature interval. Thus, the CR signal constituted well resolved lines, which is essential for the analysis of the CR line shape[19].

The two investigated orbits ζ and ψ have an effective mass that is minimal with respect to p_H[22,23] (p_H is the projection on the particle momentum on the direction of the magnetic field), and the observed lines were therefore analyzed in accordance with the corresponding formula for a resonant increment to the HF conductivity:

$$\Delta\sigma \approx A\left(\frac{-i\omega\tau}{1+i\mu}\right)^{1/2}, \qquad (2)$$

where A is a constant for the given group of electrons, $\omega = 2\pi f$, τ is the relaxation time, $\mu = \omega\tau(H - H_n)/H_n$, $H_n = m^*c\omega/en$, e is the electron charge, and c is the speed of light in vacuum.

Taking into account the smallness of $\Delta\sigma(H)$ in comparison with $\sigma(0)$, and separating the real and imaginary parts with allowance for the complex character of the piece, we can obtain expressions for $\Delta R(H)$ and $\Delta X(H)$ at resonance. Differentiation with respect to H yielded expressions for dR/dH and dX/dH, which were tabulated with a computer. The experimental plots were reduced with the aid of these tables by selecting the two parameters $\omega\tau$ and H_n, which ensured agreement of the calculated line counter with the plot. The points in Fig. 2 show the CR lines calculated in this manner. As indicated in[8], when working with a strip resonator of low Q one usually registers a signal proportional to the sum dR/dH + βdX/dH or dX/dH + βdR/dH, depending on the measurement method, with $|\beta| < 1$ (usually $|\beta| \approx 0.1$–0.3). At 75.9 GHz we registered a signal proportional to dR/dH, and the admixture of the other component of the impedance was small ($\beta < 0.1$) and was disregarded. The accuracy with which $\omega\tau$ was determined was 8–10%, and the resonant value of the magnetic field H_n was obtained with accuracy ~0.1%.

Figure 3 shows the relative changes of the effective masses of the electrons and holes in lead as a function of the square of the temperature, measured at different frequencies. The solid lines in these figures were drawn by least squares through points obtained at 75.9 GHz; the measurements and other frequencies can be described, within the limits of the measurement errors, by the same straight lines (see the table).

Figure 4 shows the values of the reciprocal relaxation-times of the electrons and holes in lead, obtained in measurements at frequencies 9.25 and 19.2 GHz, as functions of T^3, while Figs. 4 and 5 show the same for 75.9 GHz. The solid lines in Fig. 4 and the dashed lines in Fig. 5 are straight lines approximating the experimental points in accordance with the law

$$\tau^{-1} = \tau_0^{-1} + aT^3. \qquad (3)$$

The obtained temperature dependences of the relaxation time, which are connected with the electron-phonon interaction, are given in the table. At $T \lesssim 2$°K, the experimental points of Fig. 5 are so arranged as if the coefficient a were to increase with decreasing temperature (we note that hf = ke 3.64°K at f = 75.9 GHz, where h is Planck's constant, k is Boltzmann's constant, and consequently hf > kT in this region). This change of $\tau^{-1}(T)$ can be described by introducing into the approximating polynomial terms with lower powers of T. The experimental points in the insert of Fig. 5 show the experimental points plotted against the square of the temperature at $T \lesssim 2.5$°K. We see that a relation of the type (3) (dashed) describes the observed values of τ^{-1} worse than the solid curve, which was obtained by least squares and represents the function

$$\tau^{-1} = \tau_0^{-1} + bT^2 + aT^3. \qquad (4)$$

Introduction of the term bT^2 has decreased the mean-squared deviation of the point from the curve (4) by a factor of 2 in comparison with the curve described by Eq. (3). The values of a and b are determined in this case with a large error, owing to the scatter of the experimental point. Approximation by means of the polynomial (4) yields for electrons:

$$\tau_e^{-1} = (1.39 \pm 0.08)\cdot 10^9 + (2.3 \pm 0.8)\cdot 10^8 T^2 + (0.75 \pm 0.25)\cdot 10^8 T^3, \text{ sec}^{-1}.$$

It can be seen from Fig. 4 that at $T < 2$°K (f = 75.9 GHz) the plot of $\tau^{-1}(T)$ for holes also tends to have a larger slope.

DISCUSSION OF RESULTS

We use the following expression for the resonant part of the high-frequency conductivity, as obtained by Sher and Holstein[26] (see also[24]) and an analysis of CR high frequencies $\omega \sim \omega_D$ for the model of a metal with a spherical Fermi surface:

$$\sigma(\omega) = \int_{-\infty}^{\infty} d\varepsilon \frac{f(\varepsilon) - f(\varepsilon+\omega)}{\omega} \operatorname{cth}\pi\left[-i\frac{\omega + M(\varepsilon) - M(\varepsilon+\omega)}{\omega_c} + \frac{\Gamma(\varepsilon)+\Gamma(\varepsilon+\omega)}{\omega_c}\right]; \qquad (5)$$

here ϵ is the quasiparticle energy reckoned from the Fermi level, ω is the frequency of the measuring field, $\omega_c = eH/m_b c$, and $M(\epsilon, T)$ and $\Gamma(\epsilon, T)$ are the real and imaginary parts of the complex function $\Sigma(\epsilon, T) = M(\epsilon, T) - i\Gamma(\epsilon, T)$, which determines the change of the energy spectrum of the electron in the system of interacting electrons and phonons[1,2,7]. Here $\Gamma(\epsilon, T)$ is the width of the level with energy ϵ, and is directly connected with the lifetime on the corresponding quasiparticle state: $\hbar/\tau = 2\Gamma(\epsilon, T)$, while the derivative $-dM/d\epsilon = \lambda(\epsilon, T)$ determines the renormalization of the electron velocity on the Fermi surface $v_F^* = v_F/(1+\lambda)$ and of the effective mass $m^* = m_b(1+\lambda)$.

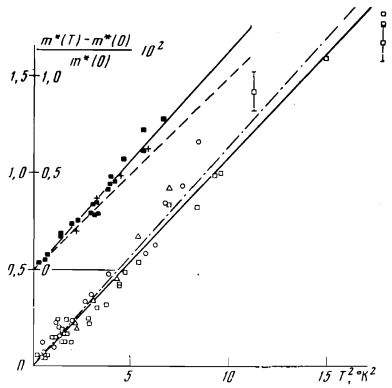

FIG. 3. Dependence of $\Delta m^*(T^2)/m^*(0)$ for the electron orbit ξ: ○–Pb I, H ∥ [110], f = 19.2 GHz; △–Pb II, ∠H, [01̄1] ≃ 2°, f = 9.25 GHz; □–Pb II, ∠H, [01̄1] ≃ 7°; f = 75.9 GHz. The solid line is drawn through the experimental points, the dash-dot line shows the theoretical relation [24] for $\lambda = 1.5$. The plot of $\Delta m^*(T^2)/m^*(0)$ for the hole orbit ψ is shown shifted upwards: +–Pb II, ∠H, [01̄1] ≈ 2°, f = 9.25 GHz; ■–Pb II, ∠H, [011] ≈ 7°; f = 75.9 GHz. The solid line is drawn through the experiments points and the dashed one shows the theoretical relation [24] for $\lambda = 1$.

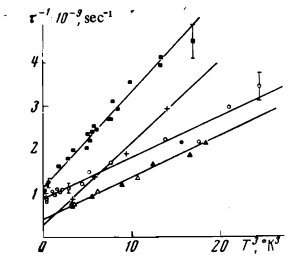

FIG. 4

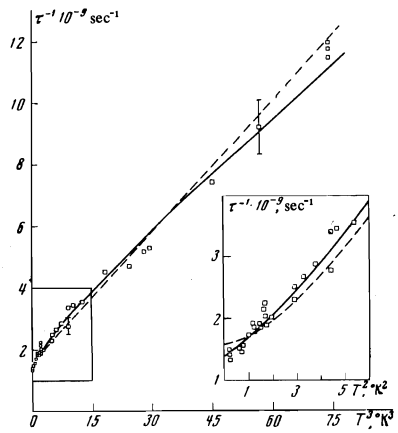

FIG. 5

FIG. 4. Plot of $\tau^{-1}(T^3)$ for the electron orbit ξ: ○–Pb I, H ∥ [110], f = 19.2 GHz; △–Pb II, ∠H, [01̄1] ≈ 2°, f = 9.25 GHz; △–Pb II, ∠H, [01̄1] ≈ 20°, f = 9.25 GHz and for the hole orbit ψ: +–Pb II, ∠H, [01̄1] ≈ 2°, f = 9.25 GHz; □–Pb II, ∠H, [011] ≈ 7°, f = 75.9 GHz. Straight lines–approximation of the experimental points in accordance with formula (3).

FIG. 5. Plot of $\tau^{-1}(T^3)$ for the electron orbit ξ: □–Pb II, ∠H, [01̄1] ≈ 7°, f = 75.9 GHz. Insert–plot of $\tau^{-1}(T^2)$. Dashed–approximation by formula (3), solid–by formula (4).

	Electron orbit ξ	Hole orbit ψ
$m^*_{exp}(0)/m_0$ at H ∥ [01̄1]	0.537±0.001	1.120±0.002
m_b/m_0, calculation [25]	0.22	0.56
$\lambda(0)$	1.44	1.0
$\Delta m^*(T)/m^*(0)$	$(1.1\pm0.1)\cdot10^{-3}T^2$	$(1.14\pm0.1)\cdot10^{-3}T^2$
$\Delta\lambda(T)/\lambda(0)$	$(1.86\pm0.2)\cdot10^{-3}T^2$	$(2.28\pm0.2)\cdot10^{-3}T^2$
τ_{ep}^{-1}, sec⁻¹ f = 9.25 GHz	$(1.0\pm0.1)\cdot10^8T^3$	$(1.9\pm0.2)\cdot10^8T^3$
τ_{ep}^{-1}, sec⁻¹ f = 75.9 GHz	$(1.4\pm0.2)\cdot10^8T^3$	$(2.2\pm0.2)\cdot10^8T^3$

In the limiting case of low frequencies $\omega \ll \omega_D$, using the relation

$$\frac{f(\varepsilon)-f(\varepsilon+\omega)}{\omega} \approx -\frac{df}{d\varepsilon} \approx \delta(\varepsilon),$$

we can reduce (5) to the form

$$\sigma(\omega) = \operatorname{cth}\pi\left[-i\frac{\omega}{\omega_c}\left(1-\frac{dM(0)}{d\varepsilon}\right)+\frac{2\Gamma(0)}{\omega_c}\right] = \operatorname{cth}\pi\left[-i\frac{\omega}{\omega_c^*}+\frac{1}{\omega_c^*\tau^*}\right]; \quad (6)$$

$$\omega_c^* = \frac{eH}{m_b(1+\lambda)c}, \quad \frac{1}{\tau^*} = \frac{2\Gamma(0)}{1+\lambda}.$$

Analyzing the shape of the CR line, Chambers[19] started from an expression of the type (6) for the conductivity. It is seen from this expression that in low-frequency CR, the measured line position yields the renormalized effective mass

$$m^*(T) = m_b[1+\lambda(0, T)],$$

while the line width yields the relaxation time $\tau^*(0, T)$ on the Fermi surface. Inasmuch as $\Gamma(0, 0) = 0$ on the Fermi surface, it is necessary to introduce also the relaxation time τ_0 connected with scattering by the crystal defects and impurities.

Theoretical calculations of $\lambda(\epsilon, T)$ and $\Gamma(\epsilon, T)$ for real metals, carried out in recent years[7,24,27], were mainly performed by transforming the complicated integral with respect to the momentum which determines $\Sigma(\epsilon, T)$ to an integral with respect to the energies. In this case the quantities averaged over the Fermi surfaces are given by

$$\lambda(0, T) = 2\int_0^\infty \frac{\alpha^2(\omega)F(\omega)}{\omega}\theta\left(\frac{\omega}{T}\right)d\omega, \quad (7)$$

$$\Gamma(0, T) = 2\pi\int_0^\infty \alpha^2(\omega)F(\omega)[f(\omega)+N(\omega)]d\omega, \quad (8)$$

where $\alpha^2(\omega)$ is the square of the matrix element of the electron-phonon interaction, $F(\omega)$ is the phonon density of states, and

$$\theta\left(\frac{\omega}{T}\right) = \int_{-\infty}^{\infty} d\varepsilon \frac{df}{d\varepsilon}\frac{\omega^2}{\varepsilon^2-\omega^2}$$

is a universal function introduced by Grimvall[7] and by Allen and Cohen[26]; in the low-temperature limit we have

$$\theta\left(\frac{\omega}{T}\right) \approx 1+\frac{\pi^2}{3}\left(\frac{kT}{\hbar\omega}\right)^2,$$

and this determines the law governing the variation of $\lambda(T)$; $f(\omega)$ and $N(\omega)$ in (8) are the Fermi and Bose distribution functions.

The function $\alpha^2(\omega)F(\omega)$, averaged over the Fermi surface, was reconstructed for lead from tunnel experiments in the superconducting state[4]. According to[4]

$$\lambda(0) = 2\int_0^\infty \frac{\alpha^2(\omega)F(\omega)}{\omega}d\omega = 1.5,$$

but a comparison on the effective mass measured in[3] and those refined in the present paper, with those calculated by the 4-APW model[22] are using a nonlocal pseudopotential[25], points to a small anisotropy of λ on the Fermi surface. Of particular importance is the dif-

ference for the carriers in the different bands (see the table).

The dash-dot and dashed curves in Fig. 3 are plots of $m^*(T)$ in lead, calculated by Allen[24] using the function $\alpha^2(\omega)F(\omega)$ from the paper of McMillan and Rowell.[4] The agreement between theory and experiment should be regarded as good, particularly in view of the anisotropy of λ. Carbotte and co-workers[28] have concluded that the main contribution to the anisotropy of λ in aluminum and in zinc is made by the anisotropy of the phonon spectrum, but no such calculations have been made for lead so far.

As to the calculations of the relaxation time in[7,24], according to (8), neglecting the Debye spectrum for the phonons and, recognizing that $\alpha^2(\omega)F(\omega) \propto \omega^2$, we can show that $\Gamma(0, T) \propto T^3$, in agreement with experiment. The coefficient of T^3 can be reliably determined only by a detailed analysis of the matrix elements of the electron-phonon interaction and the anisotropy of the sound velocities in the crystal.

Allen[24] calculated on the basis of (8) the quantity $\tau_{ep}^{-1} \approx 4.6 \times 10^8\, T^3\ \mathrm{sec}^{-1}$ for lead (at $\lambda = 1.5$ and $\alpha^2(\omega)F(\omega)$ from[4]); this result should be compared with the experimental values in the table, multiplied by $1 + \lambda = 2.5$ (the need for introducing the factor $1 + \lambda$ in the determination of τ^{-1} from expression (5) was pointed out by Guy[29]).

From experiments on the influence of pressure on the Fermi-surface sections areas determined from the de Haas–van Alphen effect we can estimate the diagonal components of the deformation-potential tensor, averaged over the orbit. The same components determine the matrix element of the interaction of the electron with long-wave longitudinal phonons. According to[25], the orbit ψ is more sensitive to the lattice deformation, from which we can conclude that the probability of scattering by phonons should be higher for holes of the orbit ψ than for electrons of the orbit ζ. No quantitative estimates can be made, since we do not know the off-diagonal components of the deformation-potential tensor, which determine the matrix elements of the interaction with the transverse phonons, which in turn make a large contribution to scattering in lead.

When the frequency is increased, electrons located at a distance ω over the Fermi surface begin to take part in the CR (the main contribution is made in this case by electrons located at a distance $\omega/2$ from the Fermi surface). By virtue of the $\lambda(\epsilon, T)$ and $\Gamma(\epsilon, T)$ dependences, the effective mass and the relaxation time, measured by the CR method, should depend on the frequency[26]: as $T \to 0$, we have

$$\Delta m^* / m^* \infty \omega^2, \quad \tau_{ep}^{-1} \infty \omega^3.$$

The $\tau_{ep}(\omega)$ dependence was observed in bismuth at 10–135 GHz[30]. The $m^*(\omega)$ and $\tau_{ep}(\epsilon)$ dependences in mercury and lead[29,31] were observed at much higher frequencies, 135–456 GHz. In our experiments, at 75.9 GHz, the $m^*(\omega)$ dependence does not yet come into play, but the plot of the function $\tau_{ep}^{-1}(T)$ is steeper than at lower frequencies, this being a manifestation of the $\tau_{ep}(\omega, T)$ dependence.

Allen[24] cites an expression with the aid of which it is possible to analyze the character of the $\tau_{ep}(\omega, T)$ dependence:

$$\Gamma(\varepsilon, T) = \pi \int_0^\infty d\omega'\, \alpha^2(\omega') F(\omega') \{1 - f(\varepsilon - \omega') + 2N(\omega') + f(\varepsilon + \omega')\}. \quad (9)$$

As $\epsilon \to 0$, it goes over, naturally, into (8). The relaxation time, which determines the CR line width, is equal to

$$\tau^{-1}(\varepsilon) = \frac{\Gamma(\varepsilon) + \Gamma(\varepsilon + \omega)}{1 + \lambda},$$

as follows from (5). Allen averages over ϵ in formula (5) of[24] by simply integrating the argument of the hyperbolic cotangent, as the result of which $\lambda(\omega, T)$ at $\tau^{-1}(\omega, T)$ are significantly higher than the values measured in the experiment. From the symmetrical form of the function $f(\epsilon) - f(\epsilon + \omega)$, which allowance for the fact that $\tau^{-1}(\epsilon) = [\Gamma(\epsilon) + \Gamma(\epsilon + \omega)]/(1 + \lambda)$ and increases rapidly with ϵ, it follows that the main contribution to the observed resonance is made by the transition between levels that are symmetrically disposed relative to the Fermi level[3], i.e., $\epsilon = -\omega/2$. This is illustrated in Fig. 6 by means of the CR line shapes calculated for us for the case of a quadratic spectrum: the solid line shows the CR line shape calculated after Chambers[19] under the assumption that

$$\tau^{-1} = \frac{\Gamma(-\omega/2) + \Gamma(\omega/2)}{1 + \lambda}, \quad (10)$$

with Γ calculated numerically from formula (9). The dashed curve is the same line averaged over ϵ in accordance with (5). We see that the $\omega\tau$ determined from the dashed curve exceeds by 50–20% the same parameter calculated under the assumption (n).

Calculations of the function $\tau_{ep}(\omega, T)$ performed on the basis of (9) and (10) with allowance for $\alpha^2(\omega)F(\omega) \propto \omega^2$ have shown that if our data at 9.25 GHz are taken as the low-frequency limit ($\omega \ll \omega_D$, $kT/\hbar$), then we can describe quantitatively the function $\tau_{ep}(\omega)$ at high frequencies as $T \to 0$. According to our calculations, the coefficient in the formula $\tau_\zeta^{-1} = g\omega^3$ is $g = 2.1 \times 10^{-28}\ \mathrm{sec}^2$, and its experimental value from the paper of Guy and Castaing[29] is $q = (2.2 + 0.2) \times 10^{-28}\ \mathrm{sec}^2$. However, the function $\tau(T)$ at $\hbar\omega \gtrsim kT$ agrees with our measurements only qualitatively. The crossing term $\omega^3 T^3$ in[29] cannot be explained at all. Thus, the question of the function $\tau(\omega, T)$ at temperatures $kT \sim \hbar\omega$ calls for a special theoretical study.

CONCLUSION

1. Measurements of the dependence of the effective carrier mass in lead on the temperature, carried out at frequencies 9.25–75.9 GHz in the temperature in-

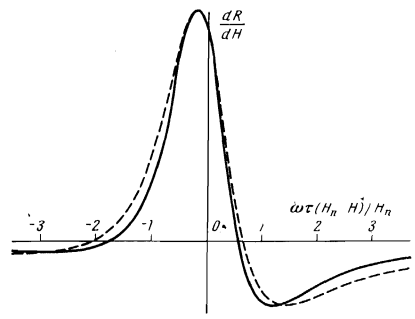

FIG. 6. CR line shape for $m^*(p_H) = \mathrm{const}$ after Chambers [19], $\omega/2\pi = 75.9$ GHz, $T = 4°K$. Solid line–under the condition (10), where Γ is calculated for (9); dashed–line shape calculated from formula (5).

terval 0.4–4.2°K and at magnetic-field directions near the two-fold axis of the crystals, has shown that the increase of the effective mass of the electrons and holes, due to the change in the value of λ, which characterizes the electron-phonon interaction, proceeds in accordance with the law $\Delta m^*/m^*(0) \propto T^2$ and reaches approximately 2% at $T = 4.2°K$. This agrees with the theoretical predictions[7,24] for the case $\hbar\omega < kT$, and also with the analogous measurements performed at higher frequencies[29] under conditions when $\hbar\omega > kT$ (in our case $\hbar\omega < kT$). On the basis of the latter comparison we can conclude that the variation of the effective mass with temperature is in first approximation independent of the variation of the effective mass with frequency.

2. We measured the temperature dependence of the time of electron and hole relaxation, due to electron phonon interaction, in lead at relatively low frequencies, before the dependence of the electron and hole lifetime on the exciting-field frequency comes into play. It turned out that the coefficient of T^3 in the $\tau_{ep}^{-1}(T)$ dependence is 1.9 times larger for holes than for electrons, i.e., in the low-frequency limit, the intensity of the electron-phonon interaction is larger for holes than for electrons. Recognizing that the effective-mass renormalization coefficient is 1.5 times larger for electrons than for holes (this coefficient is determined mainly by virtual interactions with high-frequency phonons), one should expect the electron reciprocal relaxation time to increase more rapidly with increasing frequency than this quantity for holes. Whether this is due to the change of the interaction matrix element or to the change of the geometry of the electron-phonon scattering in the anisotropy of the phonon spectrum cannot be ascertained on the basis of the available experimental data.

3. The change in the slope of $\tau^{-1}(T)$ at 75.9 GHz, observed in our experiments, and in particular the steeper dependence at $T < \hbar\omega/k$, are in agreement with the theoretical arguments that the manifestation of the $\tau(\omega)$ dependence lead to the appearance of terms with lower powers of T in the function $\tau^{-1}(T)$ (the coefficients of these terms should depend on the frequency; for example, in formula (4) we have $b \propto \omega$). In contrast to the data of Guy and Castaing[29], it is indicated in the present paper that when the frequency is increased the main contribution to the cyclotron resonance is made by electrons that are located at a distance $\hbar\omega/2$ from the Fermi surface, something that must be taken into account when a comparison is made with the theory. Using this argument, it was found that the $\tau(T)$ dependence measured at 9.25 GHz agrees with the measurements of $\tau(\omega)$ when the data of[29] are extrapolated to zero temperature. The difference in the crossing terms of $\tau(\omega, T)$ is apparently due to the change, noted in section 2, of the form of the function $\alpha^2(\omega)F(\omega)$ on going over to the higher frequencies used in[29].

The authors thank P. L. Kapitza for interest in the work, V. S. Édel'man, S. M. Cheremisin, and V. M. Pudalov for numerous useful discussions, F. Guy for the possibility of becoming acquainted with[29] prior to publication, to G. S. Chernyshev for technical help, and to the computation group of the Institute of Physics Problems for help with the calculations.

[1)]In our earlier paper [8] we indicated an erroneous orientation of the normal to the flat surface of sample Pb I, but the magnetic field was parallel to the [110] axis, so that the CR interpretation given in [8] is correct.

[2)]We are grateful to N. E. Alekseevskii and G. É. Karstens for supplying this metal from the collection of pure metals of the USSR Academy of Sciences.

[3)]This circumstance was noted in Cheremisin's paper [32].

[1] A. A. Abrikosov, L. P. Gor'kov, and I. E. Dzyaloshinskiĭ, Metody kvantovoĭ teorii polya v statisticheskoĭ fizike (Quantum field theoretical method in statistical physics), Fizmatgiz, 1962, pp. 32–37, 236–246 [Pergamon, 1965].
[2] N. W. Ashcroft and J. W. Wilkins, Phys. Lett., 14, 285 (1965). P. B. Allen and M. L. Cohen, Phys. Rev. 187, 525 (1969).
[3] R. T. Mina and M. S. Khaĭkin, Zh. Eksp. Teor. Fiz. 45, 1304 (1963) [Sov. Phys.-JETP 18, 896 (1964)].
[4] W. L. McMillan and J. M. Rowell, Superconductivity, ed. by R. D. Parks, Marcel Dekker Inc., New York (1969), p. 561. N. V. Zavaritskii, Usp. Fiz. Nauk 108, 241 (1972) [Sov. Phys.-Usp. 15, 608 (1973)].
[5] G. M. Éliashberg, Zh. Eksp. Teor. Fiz. 43, 1105 (1962) [Sov. Phys.-JETP 16, 780 (1963)].
[6] G. Grimvall, J. Phys. Chem. Sol., 29, 122 (1968).
[7] G. Grimvall, Phys. kondens. Materie, 9, 283 (1969).
[8] I. Ya. Krasnopolin and M. S. Khaĭkin, ZhETF Pis. Red. 12, 76 (1970) [JETP Lett. 12, 54 (1970)].
[9] P. Goy, Phys. Lett., 31A, 584 (1970); Phys. Lett., 32A, 474 (1970).
[10] R. G. Poulsen and W. R. Datars, Solid State Comm., 8, 1969 (1970).
[11] J. J. Sabo, Jr., Phys. Rev., B1, 1325 (1970).
[12] P. Goy and B. Castaing, Proc. of the LT 13 Conf., Colorado, 1972.
[13] R. A. Herrod and R. G. Goodrich, Phys. Lett., 33A, 331 (1970).
[14] M. S. Khaĭkin, S. M. Cheremisin, and V. S. Édel'man, Prib. Tekh. Eksp. No. 4, 225 (1970).
[15] M. S. Khaĭkin, Prib. Tekh. Eksp. No. 3, 95 (1961).
[16] V. A. Yudin, Prib. Tekh. Eksp. No. 6, 188 (1967).
[17] I. Ya. Krasnopolin, V. I. Voronin, and M. S. Khaĭkin, Abstracts of papers from 15th Conference on low temperature physics, Tbilisi, 1968 (in Russian), p. 67.
[18] V. I. Voronin, Prib. Tekh. Eksp. No. 5, 159 (1972).
[19] R. G. Chambers, Proc. Phys. Soc. 86, 305 (1965). R. G. Chambers, translation in: Fizika metallov (Metal physics), 1, Electrons, Mir, 1972, p. 252.
[20] M. S. Khaĭkin, Usp. Fiz. Nauk 96, 409 (1968) [Sov. Phys.-Usp. 11, 785 (1969)].
[21] B. E. Meĭerovich, Zh. Eksp. Teor. Fiz. 58, 324 (1970) [Sov. Phys-JETP 31, 175 (1970)].
[22] J. R. Anderson and A. V. Gold, Phys. Rev., 139A, 1459 (1965).
[23] K. Sh. Agababyan, R. T. Mina, and V. S. Pogosyan, Zh. Eksp. Teor. Fiz. 54, 721 (1968) [Sov. Phys.-JETP 27, 384 (1968)].
[24] P. B. Allen, Proceedings of the LT 12 Conference, Kyoto, 1970, ed. by E. Kanda, Keigaku Publishing Co., Tokyo, p. 517.
[25] J. R. Anderson, W. J. O'Sullivan, and J. E. Shirber, Phys. Rev., B5, 4683 (1972).
[26] H. Sher and T. Holstein, Phys. Rev., 148, 598 (1966).
[27] P. B. Allen and M. L. Cohen, Phys. Rev., B1, 1329(1970).
[28] C. R. Leavens and J. P. Carbotte, Solid State Comm., 9, 75 (1971). P. T. Truant and J. P. Carbotte, Solid State Comm., 9, 1621 (1971).
[29] P. Goy and B. Castaing, Preprint, 1972, to be published.

[30]S. M. Cheremisin, V. S. Edel'man, and M. S. Khaĭkin, Zh. Eksp. Teor. Fiz. 61, 1112 (1971) [Sov. Phys.-JETP 34, 594 (1972)].
[31]P. Goy and G. Weisbush, Phys. Rev. Lett., 25, 225 (1970).
[32]S. M. Cheremisin, ZhETF Pis. Red. 16, 186 (1972) [JETP Lett. 16, 131 (1972)].

Translated by J. G. Adashko
189